Received: 13 January 2021 | Revised: 16 August 2021 | Accepted: 23 August 2021

DOI: 10.1002/jsde.12548

ORIGINAL ARTICLE

AOCS WILEY

Effect of surfactant concentration on the hydrophobicity of polydisperse alkyl ethoxylates

Edgar Acosta[1] | **Sanja Natali**[2]

[1]Department of Chemical Engineering and Applied Chemistry, University of Toronto, Toronto, Ontario, Canada

[2]Chemical Intermediates, ExxonMobil Chemical Company, Houston, Texas, USA

Correspondence
Edgar Acosta, University of Toronto, Department of Chemical Engineering and Applied Chemistry, 200 College Street, Toronto, ON, M5S 3E5, Canada.
Email: edgar.acosta@utoronto.ca

Abstract

The effect of ethylene oxide number (EON) polydispersity on the phase behavior of alkyl ethoxylates has been well documented in the surfactant literature. These previous studies show that polydisperse alkyl ethoxylates appear more hydrophilic as the surfactant concentration decreases or as the oil-to-water ratio increases. This becomes a troubling issue considering that most surfactant formulations undergo dilution during use, and they experience a wide range of water-to-oil volume ratios. Within the hydrophilic–lipophilic difference framework, the surfactant hydrophobicity is assessed via the sigma (σ) term (also known as the characteristic curvature or Cc). In this work, the effect of surfactant concentration on the apparent value of sigma (σ_{app}) is evaluated as a function of surfactant concentration. The experimental observations are then explained using a bifunctional model for alkyl ethoxylates that consider the dual nature of polar oils (free alcohol and low EON ethoxymers) as surfactants and as oil components. A segregation-based model and a partition-based model are implemented to account for the distribution of the ethoxymers in the surfactant pseudophase and the oil phase. Combining these distribution models with the bifunctional model and a group contribution model for sigma, one can predict the σ term versus surfactant concentration for a given water/oil ratio, starting from the EON distribution of the surfactant. The practical applications of the model are discussed.

KEYWORDS
alkyl ethoxylates, characteristic curvature, HLD, microemulsions, phase behavior, sigma

INTRODUCTION

Alkyl ethoxylates involve a family of surfactants with a hydrocarbon (alkyl) group connected to a poly(ethylene oxide) (EO) group. The most common alkyl ethoxylates are alcohol ethoxylates (AEs) produced by the reaction between fatty alcohols and EO using a catalyst, typically KOH (Rosen & Kunjappu, 2012). The market share of alkyl ethoxylates has been growing since their introduction due to their mildness (as compared to ionic surfactants), their low foaming (desirable in horizontal washing machines), their tunability (by changing the chain length and average degree of ethoxylation), their compatibility with enzymes and polymers, and their ability to adapt to a wide range of electrolyte concentrations (Marketsandmarkets, 2020; Rosen & Kunjappu, 2012).

The ethoxylation catalyst used, the reaction conditions, and the target degree of ethoxylation (average number of EOs in the chain) determine the average and standard deviation of the number of EO groups per alkyl chain, as well as the fraction of free (unreacted) alcohol. The polydispersity index (PDI) is often used to quantify the polydispersity (ratio between weight fraction-averaged molecular weight and mole-fraction-averaged molecular weight). For a monodisperse surfactant PDI ~1, and PDI >1 for more polydisperse products.

High PDI values in AEs have several practical implications. First, the cloud point tends to be lower than that of a more monodisperse product (Goe, 1998). For monodisperse AEs, the best detergency tends to be obtained when the temperature of the washing approaches the phase inversion temperature (PIT) of the surfactant–oil (stain)–water (SOW) system. In general, any condition leading to the phase inversion point of the SOW system tends to improve the detergency of

the formulation (Boza-Troncoso & Acosta, 2019; Thompson, 1994; Tongcumpou et al., 2003).

The most practical method to identify the phase inversion conditions for a SOW system is via the hydrophilic–lipophilic difference (HLD) framework (Salager, 1977, 2000; Salager et al., 2000). The HLD framework consists of a set of two empirical equations (one for ionic surfactants, one for nonionic surfactants) that relate the condition of phase inversion (HLD = 0) to the temperature of the system (T), the salinity of the aqueous environment (S, often expressed in g NaCl/100 ml), and the hydrophobicity of the oil phase, expressed in terms of equivalent alkane carbon number (EACN). For linear alkanes with 5 or more carbons, the EACN is simply the number of carbons in their chain length, but for other oils, it is a value that is determined experimentally via phase inversion studies. The original empirical correlations for ionic surfactants were introduced in Salager's PhD dissertation (Salager, 1977). The correlations contained a sigma (σ) term that accounted for the hydrophobic nature of the surfactant. The physical significance of the σ term (also noted as β for nonionic surfactants) has been interpreted as the characteristic curvature (Cc) of the surfactant (Acosta et al., 2008).

Salager's formulation correlations appear in early publications under various names but finally settled on HLD, interpreting the HLD as the normalized difference between the chemical potential of the surfactant in the aqueous phase and the oil phase (Salager et al., 2000, 2013). The HLD for nonionic surfactants is (Salager et al., 1979, 2000, 2005):

$$\mathrm{HLD} = b \cdot S - k \cdot \mathrm{EACN} + c_T(T - 25^{\circ}\mathrm{C}) + \sigma. \quad (1)$$

The term $b{\cdot}S$ expresses the salting-out effect, thus "b" depends on the salt used. For sodium chloride, $b = 0.13$ when S is expressed in g NaCl/100 ml. The value of "k" can range from 0.05 (for extended surfactants) to 0.25 (for some cationic surfactants), but more often ranges from 0.15 to 0.17. The term c_T $(T - 25^{\circ}\mathrm{C})$ reflects the fact that increasing the temperature tends to dehydrate alkyl ethoxylate surfactants, making them more hydrophobic. For alkyl ethoxylates, $c_T \sim 0.06^{\circ}\mathrm{C}^{-1}$.

Figure 1 presents a comparison between values of σ calculated from a σ-Griffin's hydrophilic-lipophilic balance (HLB) correlation presented in the literature for monodisperse AEs C_nE_j where "n" is the number of carbons in the hydrocarbon tail of the AEs, a value of $n = 11$ was used for Figure 1 (Acosta, 2020). The value of "j" represents the number of EO groups in the headgroup of the surfactant. The σ-Griffin's HLB correlation was constructed using Griffin's group contribution (Griffin, 1954) for $C_{8\text{-}16}E_4$ surfactants and the σ (Cc) group contribution of Acosta (2008). Even though the σ-HLB correlation was developed for a narrow range of composition, it applies to highly ethoxylated surfactants. For example,

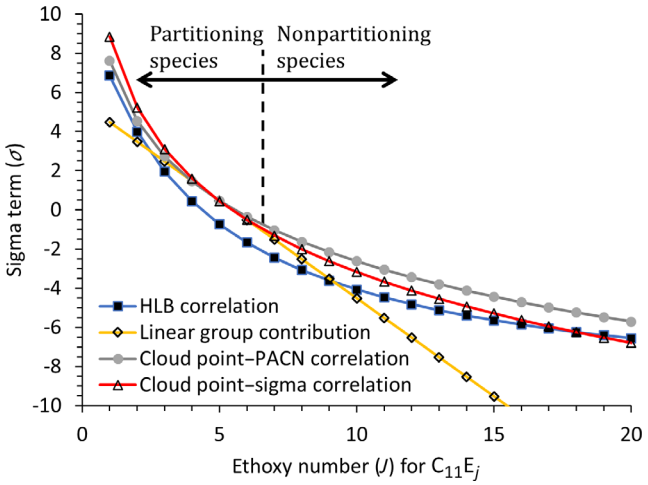

FIGURE 1 Correlations for sigma values of monodisperse alcohol ethoxylates. The hydrophile–lipophile balance (HLB) correlation was introduced by Acosta (2020) and the linear group contribution by Acosta (2008). The cloud point–preferred alkane carbon number (PACN) correlation by Aubry et al. (2020). The cloud point–σ correlation by Zarate-Muñoz et al. (2015)

the HLB of Tween 80, containing 20 EO groups, is 15. According to the correlation, $\sigma = (11.5 - \mathrm{HLB})/0.85 = (11.5\text{–}15)/0.85 = -4.1$. The σ for Tween 80 was reported to range from -3 to -3.7 by Zarate-Muñoz et al. (2016).

Another correlation shown in Figure 1 is a linear contribution group, proposed by Acosta, as $\sigma = 2.4 + 0.28{*}n - j$ (Acosta, 2008). It is important to keep in mind that this correlation was produced for systems with j values from 2 to 6 and n values from 6 to 12. To illustrate the inaccuracy of the linear approach for highly ethoxylated surfactants, one can use the linear group contribution with $n = 18$ and $j = 20$ as a preliminary estimation for Tween 80, finding $\sigma = -12.6$, which is a substantial deviation from the experimentally determined values (Zarate-Muñoz et al., 2016).

The cloud point–preferred alkane carbon number (PACN) correlation in Figure 1 uses the connection between cloud point and σ/k (PACN), and Gu's group contribution for cloud point (Aubry et al., 2020). The values of sigma presented in Figure 1 from this correlation assume $k = 0.16$. Finally, Figure 1 presents a connection between cloud point and sigma obtained by Zarate-Muñoz et al. using Huiber's group contribution for cloud point (Choi et al., 2019).

Except for the linear correlation, all other correlations in Figure 1 point to $C_{11}E_j$ surfactants with $j > 9$ approaching a plateau sigma value, deviating from the linear trend obtained with $j < 9$. Figure 1 also presents one of the central assumptions of this work, that AEs with $j < 7$ have a greater tendency to partition into the oil phase. This assumption is supported by observations of surfactant concentrations above and below critical micelle concentration (CMC) with monodisperse

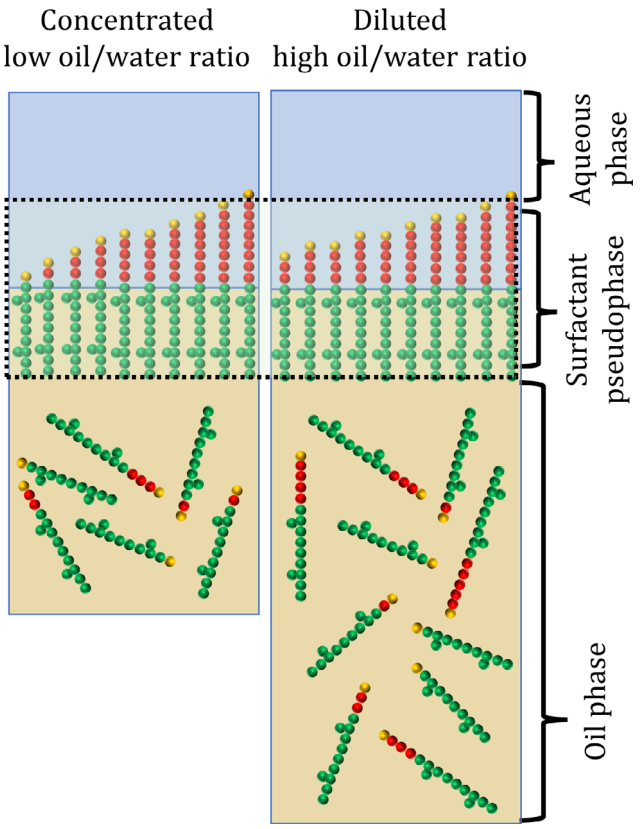

FIGURE 2 Schematic illustrating the partition of $C_{11}E_j$ surfactants in (left) concentrated environments (or low oil/water ratio) and (right) diluted environments (or high oil/water ratio). The green, red, and yellow beads represent carbon groups (CH_3, CH_2, and CH), the ethoxy group (—OCH_2CH_2—), and the hydroxyl group (—OH), respectively

ethoxylated alkylphenols. Harusawa et al. determined that above the CMC, increasing the concentration of nonylphenol (NPE) with four ethoxy groups (NPE4) in a water–isooctane system resulted in a selective partition into the oil phase (Harusawa et al., 1982). However, for NPE6 and NPE8 in the same system, any surfactant addition beyond the CMC resulted in an accumulation of the surfactant in the aqueous phase. When the researchers changed the oil phase from isooctane to cyclohexane, NPE6 accumulated in the oil phase. A similar transition around six ethoxy groups was observed by Marquez et al. (2000).

Once an aqueous polydisperse surfactant solution is set in contact with an oil phase, the more lipophilic surfactant species (having low "*j*") partition into the oil phase, changing the composition of the mixture. Figure 2 presents a schematic of this partition behavior in two cases: a concentrated surfactant solution (or a system with a low oil/water ratio) and a diluted surfactant solution (or a system with a high oil/water ratio). Comparing the low and high oil/water ratio cases in Figure 2, one realizes that in the system with less oil, there is less capacity to extract surfactant from the interface, and only a fraction of the lipophilic (low "*j*") species partition into the oil phase. Increasing the oil phase volume increases the capacity to extract more lipophilic species from the surfactant pseudophase.

Evidence of the partition behavior illustrated in Figure 2 and its impact on the hydrophobicity of the surfactant can be found in various sources (Antón et al., 2008; Goe, 1998; Kunieda & Shinoda, 1985). For example, Shinoda's phase diagrams (at constant total surfactant concentration) of temperature versus oil fraction show that, for alkylphenol ethoxylates, increasing oil fraction increases the PIT of the system (Kunieda & Shinoda, 1985). In other words, at high oil/water ratios, the surfactant mixture is more hydrophilic and requires a higher temperature to undergo phase inversion. This observation was translated into a linear relation between σ and the logarithm of the oil/water ratio (Acosta, 2008).

Antón et al. discussed the partition of AEs in detail, using schematics of changes in EO distribution after surfactant contact with the oil phase. They noted that surfactant partition is evidenced in oblique fish phase diagrams where the temperature boundaries increase in magnitude at lower surfactant concentrations. Another way in which the same effect is observed is that more hydrophobic (low average "*j*") surfactants were required to achieve phase inversion at a given temperature when the surfactant concentration was reduced. Antón et al. suggested that the ethoxymers partitioning into the oil phase are primarily those with $j < 5$ (Antón et al., 2008).

Although having monodisperse AEs would solve various phase behavior problems, the separation costs associated with producing monodisperse AEs are prohibitive for most applications. Instead, finding a way to understand the impact of AE polydispersity on phase behavior and a way to manage it is a more promising route to improve formulations containing AEs. The purpose of this work is to introduce a framework that can predict the SOW phase behavior of polydisperse AEs using the HLD framework (Equation 1) and a bifunctional model for polar oils that accounts for the surfactant and oil-like behavior of molecules such as low "*j*" AEs.

MODEL DEVELOPMENT

The segregation-bifunctional model for polydisperse AEs is summarized in the algorithm of Figure 3. The bifunctional model of polar oils was originally derived to account for the polar oil segregated at the interface and the amount that remained molecularly dissolved in the oil phase. The portion that segregated toward the interface was considered to behave as a surfactant, with a given $\sigma_{\text{polar oil}}$, and the portion dissolved in the oil was considered an oil with a given $\text{EACN}_{\text{polar oil}}$.

Before describing the details of the segregation-bifunctional model, it should be noted that the partition

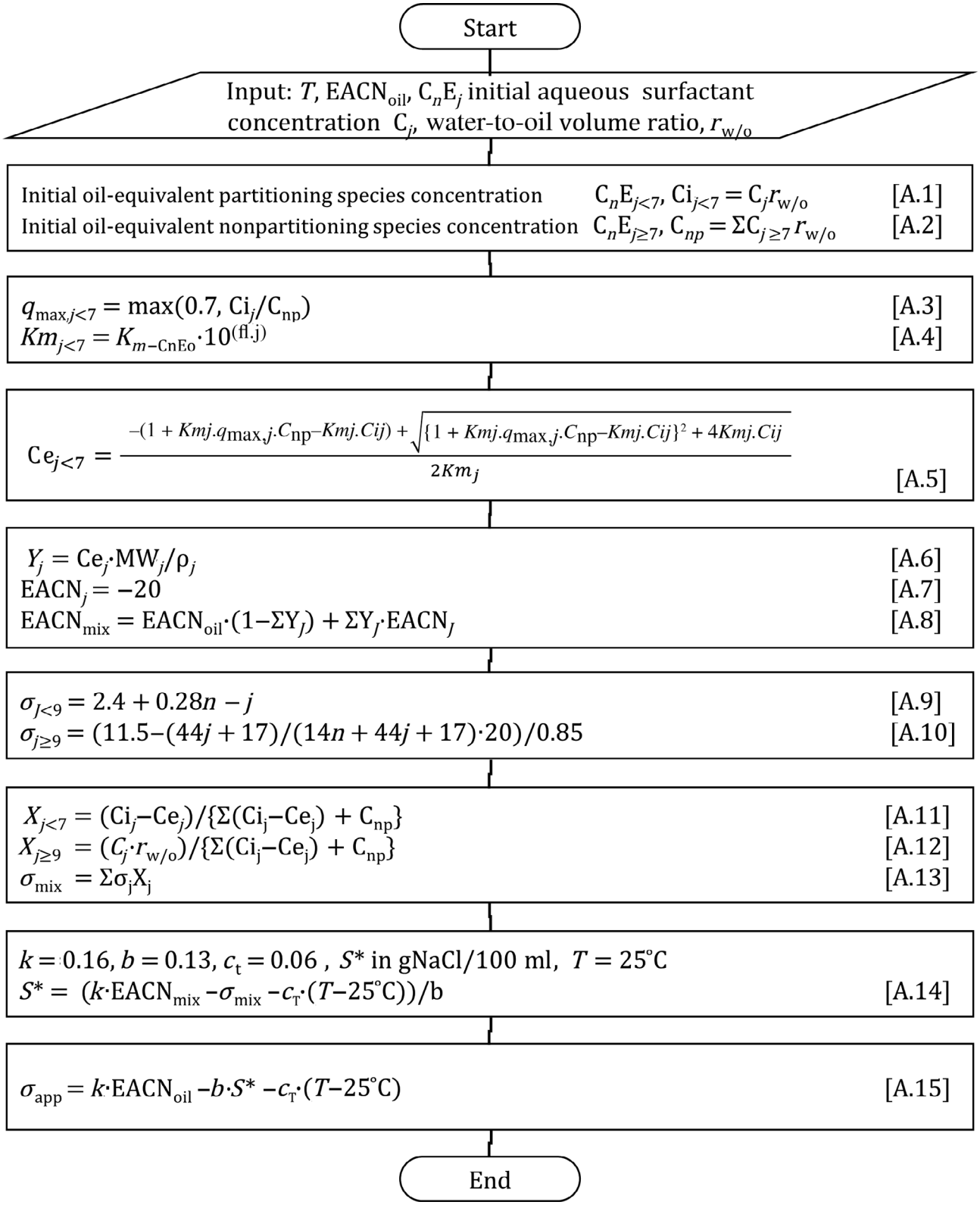

FIGURE 3 Segregation-bifunctional model algorithm for polydisperse alcohol ethoxylates

of ethoxymers has been modeled in the past considering a chain equilibrium between the micelle (the surfactant pseudophase in this work) C_nE_j composition, the C_nE_j composition of molecules dissolved in water, and the C_nE_j composition of molecules dissolved in oil (Graciaa et al., 1983, 2006; Harusawa & Tanaka, 1981;

Kibbey & Chen, 2008; Warr et al., 1983). Normally solving a partition model requires solving, simultaneously, several nonlinear equations. Section I in File S1 introduces a simplified method of implementing the partition model to calculate the oil and surfactant pseudophase composition.

In the segregation-bifunctional model, the partition of low "*j*" ethoxymers is described as a segregation phenomenon between the surfactant pseudophase, where nonpartitioning C_nE_j species are present, and the oil phase. As indicated earlier, several references point to six ethoxymers as being the point of transition between oil-partitioning and nonpartitioning surfactants (Antón et al., 2008; Graciaa et al., 1983; Harusawa et al., 1982; Márquez et al., 2000; Zarate-Muñoz et al., 2015). Therefore, the segregation model algorithm in Figure 3 considers C_nE_j species with $j < 7$ partitioning species, and species with $j \geq 7$ are nonpartitioning C_nE_j. The segregation model of Figure 3 uses as an input the initial (before setting the formulation in contact with the oil) aqueous molar concentration of the surfactant with a known ethoxy distribution (C_j in the figure) and expected water-to-oil volume ratio ($r_{w/o}$) because this is likely the information that is known to the formulator. Most formulations are aqueous solutions, most surfactant manufacturers have an ethoxy distribution for their products, or it can be obtained via standard chromatography methods, and the water-to-oil ratio applicable during the use of the product is something that the formulator needs to consider ahead of the formulation efforts. The term $C_j \cdot r_{w/o}$ in Equations (A.1) and (A.2), Figure 3, neglects the CMC of the surfactant in water; thus, the algorithm should not be used when the total surfactant concentration is close to the CMC (for the surfactants in this work, CMC <0.1 wt%). For the segregating surfactants with $j < 7$, the initial concentration in the oil phase, before segregation, is $Ci_j = C_j \cdot r_{w/o}$ (Equation A.1, Figure 3). The total oil-equivalent concentration of the nonpartitioning species is $C_{np} = \Sigma C_j \cdot r_{w/o}$ for $j \geq 7$ (Equation A.2, Figure 3). The use of oil-equivalent concentration for nonpartitioning species is simply a method to express the ratio between the moles of interfacially active species and the oil volume, in a way that facilitates the mass balance of the polar oils.

To represent the polar oil segregation of the partitioning surfactant species in the surfactant pseudophase using a Langmuir isotherm, one needs two parameters, $q_{max,j}$ and Km_j, such that $q_j = q_{max,j} \cdot Km_j \cdot Ce_j / (1 + Km_j \cdot Ce_j)$. This segregation approach was previously validated for naphthenic acid and dodecanol, used as an example of polar oils, with ionic and nonionic surfactants (Ghayour & Acosta, 2019, 2020). The segregation-bifunctional model has also been used to predict the phase behavior of cosmetic formulations for skin cleaning, including cholesterol and oleic acid as polar oils (Acosta, 2020); and to evaluate the effect of polar oils (oleic acid) in oily substrates removed with a detergent formulation based on alkyl ethoxylates (Natali & Acosta, 2019).

The term q_j in the Langmuir equation is the ratio between the moles of polar oil species segregated to the surfactant pseudophase and the moles of nonpartitioning surfactant species in the surfactant pseudophase. Therefore, $q_{max,j}$ is simply the maximum value of q when the interface is saturated with the polar oil species. The value of Km_j can be interpreted as a term proportional to the partition coefficient between the equilibrium concentration of the polar oil after segregation (Ce_j) and the oil-equivalent concentration of polar oil segregated in the surfactant pseudophase ($C_{seg,j}$). $C_{seg,j}$ can be calculated as $C_{seg,j} = q_j \cdot C_{np} = q_{max,j} \cdot Km_j \cdot Ce_j \cdot C_{np} / (1 + Km_j \cdot Ce_j)$. At low polar oil concentrations, $Km_j \cdot Ce_j << 1$, the Langmuir expression is linear, and the partition coefficient between the segregated and dissolved polar oil, $K_{seg/diss} = C_{seg,j} / Ce_j = q_{max,j} \cdot Km_j \cdot C_{np}$. Thus, $K_{seg/dis} \propto K_m$.

For partitioning polar oils, added at relatively low concentrations (often less than 20 mol%) in relation to the surfactant, previous work has found that values of q_{max} ~0.7 are appropriate for the segregation-bifunctional model (Ghayour & Acosta, 2019). However, in our preliminary simulations, we determined that if the ratio C_j/C_{np} was larger than 0.7, then using $q_{max} = 0.7$ produced an overestimation of the partition of these species. Therefore, the value of q_{max} must be considered for each species ($q_{max,j<7}$), as the maximum value between 0.7 (suitable for low $C_{j<7}$) and C_j/C_{np} (suitable for high $C_{j<7}$), as indicated in (Equation A.3, Figure 3).

The value of Km_j for each partitioning species is not a trivial number to assign. In principle, one would need to run polar oil phase behavior with the pure $C_nE_{j<7}$ species tests and a reference surfactant to fit Km_j. However, if one can obtain the value of Km_j for the alcohol ($Km_{j=0}$) and find a way to correlate the Km_j values for the rest of the partition species, much work and time could be saved. To find this correlation, one could turn to the work of Zarate-Muñoz et al. that considered the partition between AEs in water and oil, using the UNIFAC model (Zarate-Muñoz et al., 2015). Using the values of partitions presented in Zarate-Muñoz et al., Figure 4 presents the logarithm of the ratio between the partition coefficient of a C_nE_j species and the partition coefficient of the alcohol C_nE_0 (extrapolated from the values in the reference). The linear correlations obtained from Figure 4 can be turned into an expression of the form $Km_j = Km_0 \cdot 10^{(fl \cdot j)}$ (Equation A.4, Figure 3). Following the UNIFAC correlation introduced in previous work (Boza-Troncoso & Acosta, 2015; Zarate-Muñoz et al., 2015), $fl = 0.42$ (partition of molecularly dissolved species), which is consistent with experimental trends shown in numerous sources (Graciaa et al., 2006; Kibbey & Chen, 2008; Márquez et al., 2000; Salager et al., 2000).

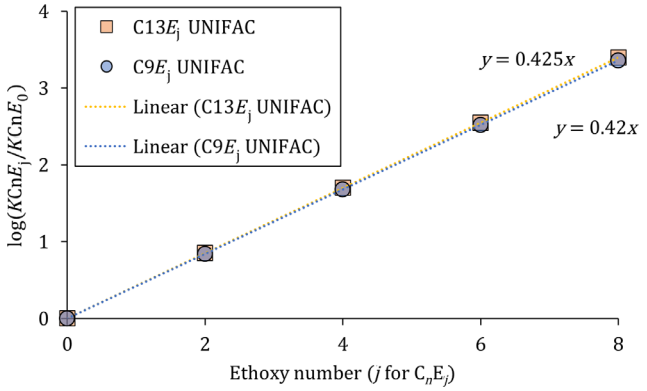

FIGURE 4 Ratio between water–oil partition coefficients of C_nE_j surfactants and free alcohol (C_nE_0) versus ethoxy group number (j) for C_9E_j and $C_{13}E_j$. Values calculated from UNIFAC simulations were obtained by Zarate-Muñoz et al. (2015)

Equation (A.5) in the algorithm of Figure 3 is the mass balance solution for the polar oil segregation, indicating what portion of the initial concentration Ci_j remains dissolved in the oil phase (Ce_j) and which portion segregates toward the surfactant pseudophase ($Ci_j - Ce_j$). Equation (A.6), Figure 3, converts the dissolved molar concentration of the partitioning species into a volume fraction in the oil (Y_j). Equation (A.7), Figure 3, presents another important simplification in the algorithm: all partitioning species have the same $EACN_{polar\ oil} = -20$. Values of EACN of fatty alcohols and fatty acids range from −9 to −80, often with large uncertainties that overlap with the value of $EACN_{polar\ oil} = -20$ (Acosta, 2020; Ghayour & Acosta, 2019, 2020). Given the large uncertainty in the EACN of polar oils, the model uses the most common value of −20, but this is an aspect that is open to re-examination. Equation (A.8), Figure 3, presents a linear mixing rule for the EACN of the oil mixture considering the volume fraction of each partitioning oil (Y_j) and the oil fraction of the nonpolar oil ($1 - \Sigma Y_j$) (Kiran et al., 2009). Equation (A.8) implies that the partitioning of the low "j" AEs affects the polar nature, thus the EACN, of the oil phase.

Equations (A.9) and (A.10), Figure 3, present group contribution equations (based on the trends of Figure 1) to calculate σ, considering the correlations presented in Figure 1. The linear trend in Figure 1 has been confirmed in the literature for j between 2 and 6 (Acosta, 2008). However, for the nonpartitioning species, the HLB-σ correlation was used given the suitability of the HLB to describe the hydrophobicity of AEs with large "j". The cloud point correlations used in the other nonlinear correlations in Figure 1 did not include experimental cloud points for large "j" numbers. It is worth mentioning that the linear correlation itself was not developed for j values of 0 and 1, so the σ calculated with these "j" values are likely overestimations of the real value of σ. For example,

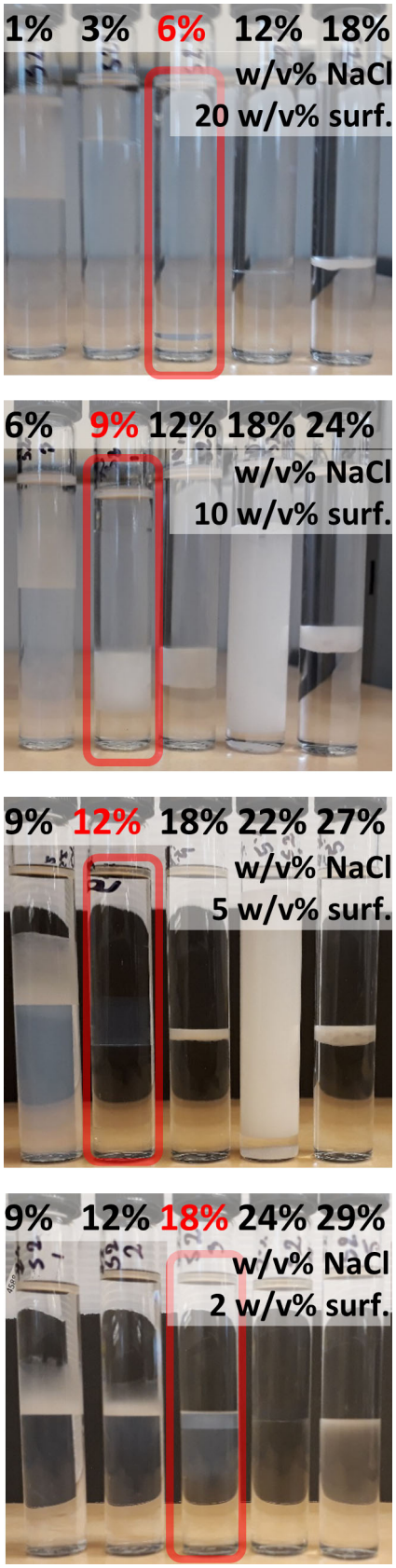

FIGURE 5 Phase behavior (salinity) scans for the $C_{11}E_{5\_NR}$–heptane–brine system at $T = 25°C$ and total initial aqueous surfactant concentration of (from top to bottom) 20, 10, 5, and 2 wt%

for dodecanol ($C_{12}E_0$), $\sigma \sim 2.0$ has been reported (Ghayour & Acosta, 2020), but the linear correlation of Equation (A.9), Figure 3, would predict $\sigma \sim 5.8$. As there are no alternative correlations for sigma values for $j = 0$ and 1, the linear correlation would be considered valid for those points.

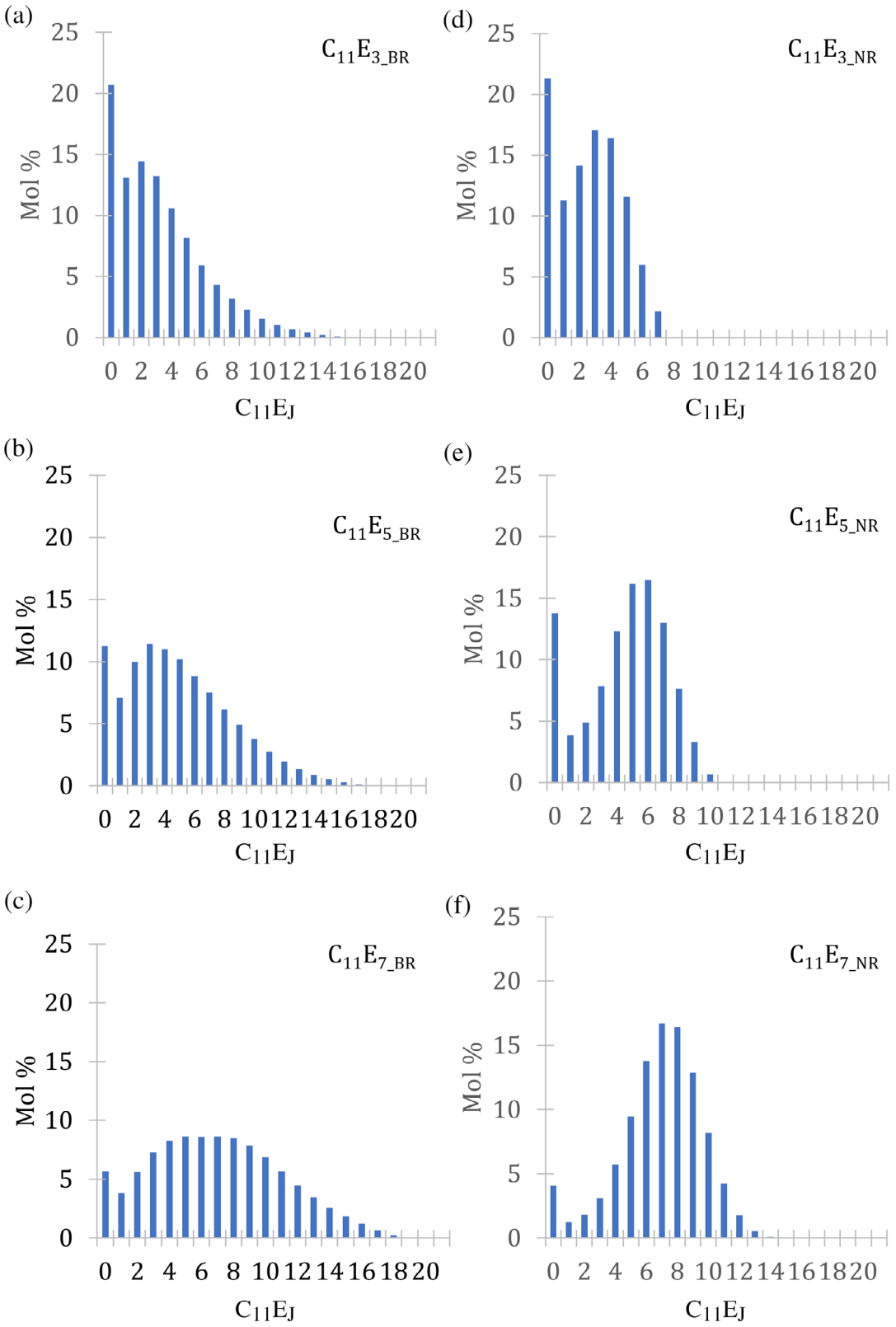

FIGURE 6 Ethoxymer (ethylene oxide) distribution (obtained via high-temperature gas chromatography) for C_{11} alcohol ethoxylates with broad range (BR) and narrow range (NR) distribution and nominal degree of ethoxylation of 3, 5, and 7

Equations (A.11) and (A.12), Figure 3, are used to calculate the molar fraction in the surfactant pseudophase of the partitioning ($X_{j<7}$) and nonpartitioning species ($X_{j\geq 7}$), respectively. The fractions were calculated using the oil-equivalent concentrations in the surfactant pseudophase of the partitioning ($Ci_j - Ce_j$) and nonpartitioning ($C_{nj}{\cdot}r_{w/o}$) species. Equation (A.13), Figure 3, calculates the mixed sigma for the mixture (σ_{mix}), and Equation (A.14), Figure 3, calculates S^* at HLD = 0 considering $EACN_{mix}$. The apparent sigma (σ_{app}) is calculated using S^*, HLD = 0, and $EACN_{oil}$ (7 for heptane) (Equation A.15, Figure 3).

In addition to the segregation-bifunctional model, some of the results include a partition-bifunctional model. This partition version of the bifunctional model obtains the composition in the surfactant pseudophase (X_j) and the concentration of all the species in the oil phase (Ce_j) via a simplified solution of the simultaneous mass balances. This simplified solution is shown in Section I of File S1. With the X_j and Ce_j values, then Equations (A.6) through (A.10) and Equations (A.13) through (A.15), Figure 3, are utilized to find the apparent sigma (σ_{app}).

The σ_{app} value is what someone would obtain experimentally by running a salinity phase scan with a surfactant, obtaining the salinity at phase inversion (S^*), and simply calculating the sigma value, assuming that the EACN of the oil is the known EACN of the nonpolar oil used in the phase scans. Figure 5 illustrates this scenario presenting the salinity scan at different total surfactant concentrations for one of the surfactants considered in this work, a narrow EO distribution $C_{11}E_{5\_NR}$. The system of Figure 5 was produced with *n*-heptane as a nonpolar oil (EACN = 7), at $T = 25^\circ$C, and using sodium chloride as the scanning electrolyte. This salt concentration increases in each tube (%wt/vol is g NaCl/100 ml aqueous phase) from left to right. The highlighted test tube corresponds to the closest tube to the phase inversion salinity (S^* or optimal salinity is the salinity where HLD = 0 and middle phases tend to be observed) where the volumes of oil and water solubilized in the middle phase are equal. For the case of 20% initial aqueous solution of $C_{11}E_{5\_NR}$, S^* ~ 6% NaCl. Considering the HLD constants for AEs listed in the algorithm of Figure 3, one would calculate σ_{app} = 0.16*7–0.13*6–0.06*(25–25) = 0.34. Similarly, for 10% $C_{11}E_{5\_NR}$ (S^* ~ 9% NaCl) one would obtain $\sigma_{app} \sim -0.05$; for 5% $C_{11}E_{5\_NR}$ (S^* ~ 12% NaCl) one would obtain $\sigma_{app} \sim -0.44$; and for 2% $C_{11}E_{5\_NR}$ (S^* ~ 18% NaCl) one would obtain $\sigma_{app} \sim -1.2$.

To test the algorithm of Figure 3 against experimental σ_{app} values, first, the value of Km_0 for the free alcohol was obtained. Then the algorithm of Figure 3 was run assuming the UNIFAC correlation for *Km*, where fl = 0.42. The fully predicted σ_{app} was then compared with the experimental σ_{app} values obtained at 20, 10, 5, and 2 wt% initial aqueous surfactant concentrations. Three different levels of ethoxylation were considered, 3 EO, 5 EO, and 7 EO, and two different distributions, one is a broad range (BR) ethoxylation and the other is a narrow range (NR) ethoxylation. The BR and NR terms refer to the difference in the degree of polydispersity, which depends on the type of catalyst used to conduct the ethoxylation of the alcohol (Rosen & Kunjappu, 2012). The similarities and differences between the predicted and experimental σ_{app} are then discussed for the six surfactants considered. All the experiments used *n*-heptane as the nonpolar oil, NaCl as the electrolyte, and $T = 25^\circ$C.

To further evaluate the bifunctional model for polydisperse AEs, the algorithm of Figure 3 is later

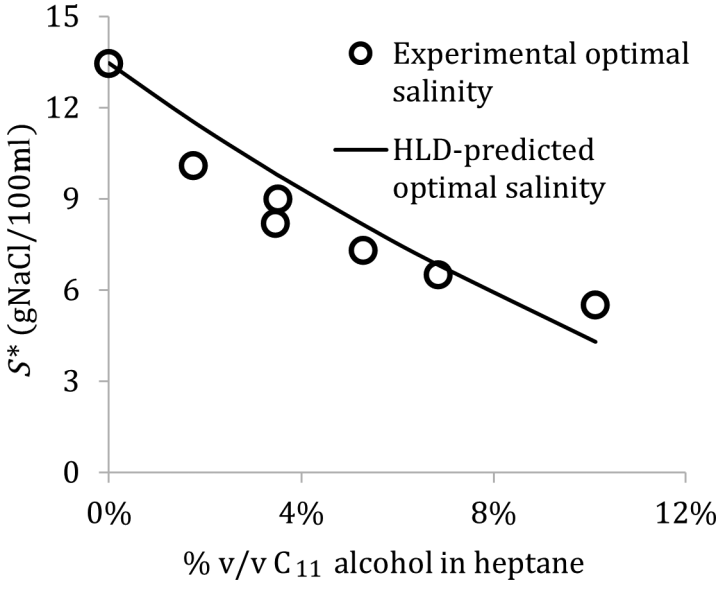

FIGURE 7 Phase inversion (optimal, S^*) salinity of systems prepared with 16 wt% C_9E_5 as reference surfactant and mixtures of C_{11} alcohol in heptane. The hydrophile–lipophile balance (HLD)-predicted (solid) line was obtained using the bifunctional model of polar oils with $\sigma_{C9E5} = -0.6$, $\sigma_{C11alcohol} = 5.5$, $EACN_{C11alcohol} = -20$, $q_{max,C11alcohol} = 0.7$, $K_{m,C11alcohol} = 0.53\ M^{-1}$

combined with the HLD–net-average curvature (HLD–NAC) model to predict "fish" phase diagrams of mixtures of monodisperse $C_{12}E_4$, $C_{12}E_6$, and $C_{12}E_8$ that Kunieda and Shinoda used to assess the fish phase diagram of polydisperse systems (Kunieda & Shinoda, 1985). To illustrate the step-by-step implementation of the algorithm of Figure 3, along with the NAC implementation, Section II of File S1 presents the sequence of calculations associated with one of the systems of Kunieda and Shinoda (1985).

MATERIALS AND METHODS

Materials

AEs with BR and NR EO distribution $C_{11}E_{3\_BR}$ (~100%), $C_{11}E_{5\_BR}$ (~100%), $C_{11}E_{7\_BR}$ (~100%), $C_{11}E_{3\_NR}$ (~100%), $C_{11}E_{5\_NR}$ (~100%), and $C_{11}E_{7\_NR}$ (~100%) were donated by ExxonMobil Chemical Company. Figure 6 presents the EO distribution for each of these surfactants, as reported by a third-party laboratory and

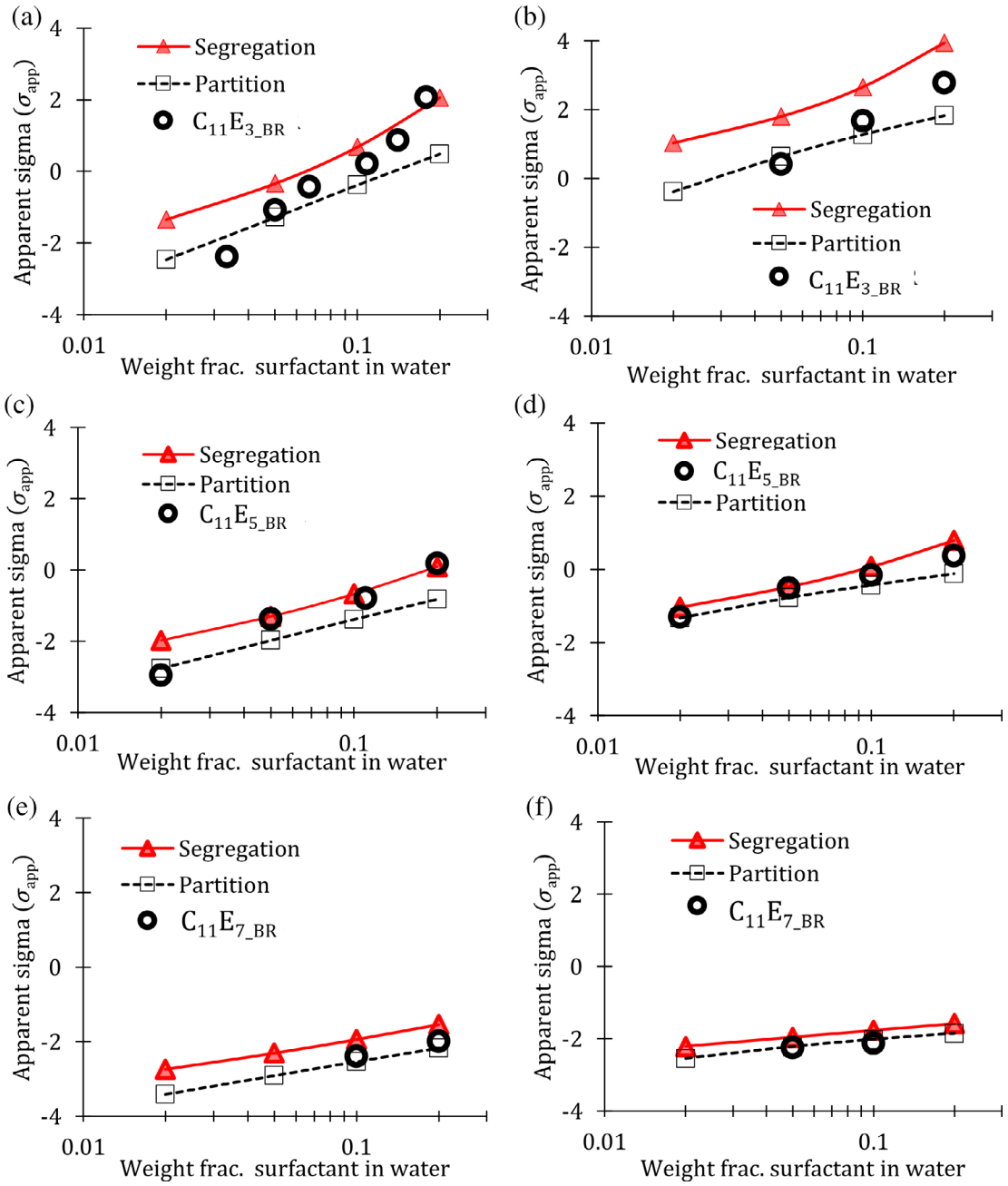

FIGURE 8 Apparent sigma values (σ_{app}) for alcohol ethoxylates (AEs) with a broad range (a, $C_{11}E_{3\_BR}$; c, $C_{11}E_{5\_BR}$; e, $C_{11}E_{7\_BR}$) and narrow range (b, $C_{11}E_{3\_NR}$; d, $C_{11}E_{5\_NR}$; f, $C_{11}E_{7\_NR}$) ethylene oxide distribution versus AE weight fraction in water. Circles represent experimental σ_{app} from salinity scans. Triangles represent σ_{app} values predicted with the segregation-bifunctional AE algorithm of Figure 3, and the squares represent the partition-bifunctional model predictions. BR, broad range; NR, narrow range

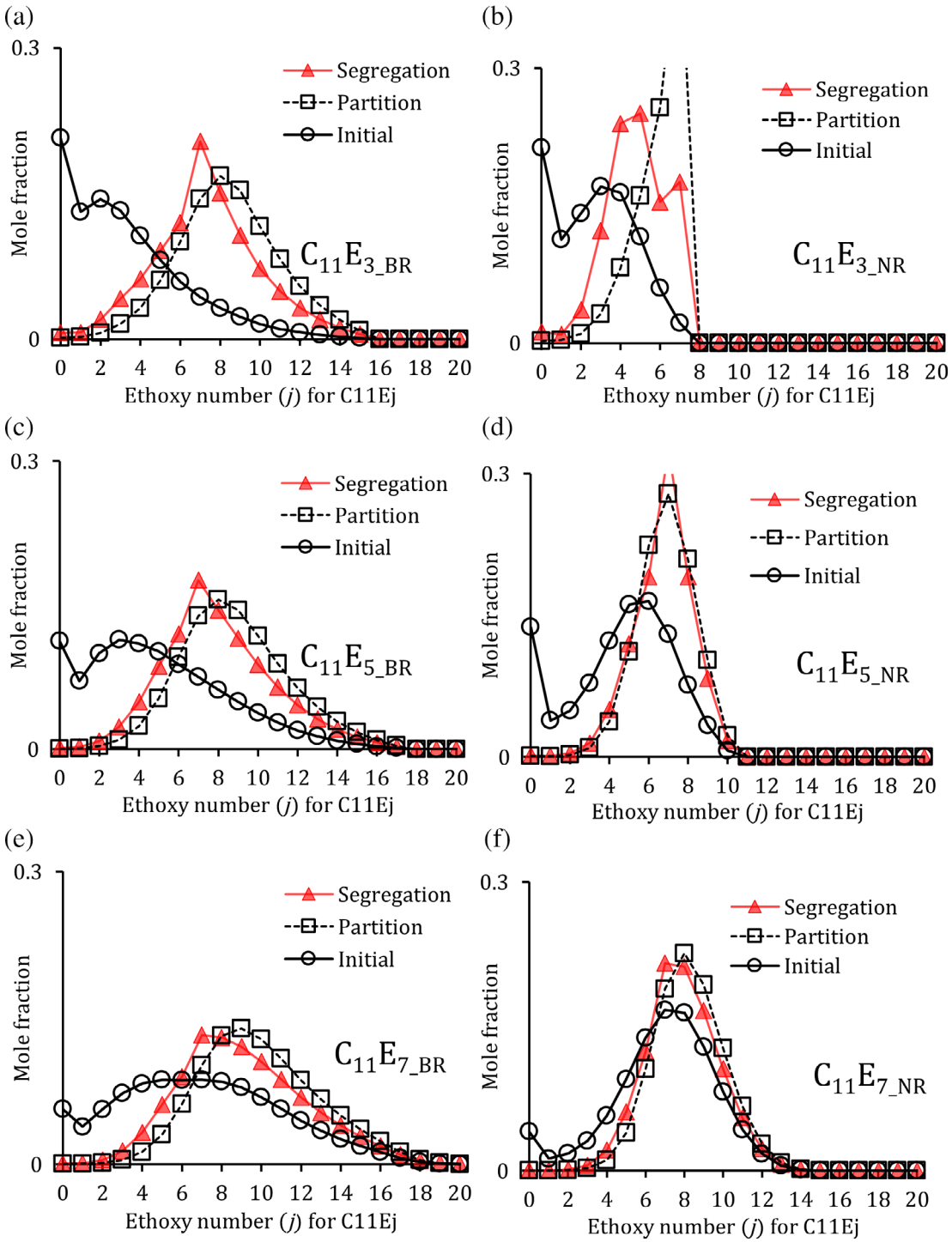

FIGURE 9 Ethoxymer (ethylene oxide) distribution of alkyl ethoxylate surfactants broad range (BR) and narrow range (NR) distribution in the surfactant pseudophase before contacting with heptane (initial, circles), and after contacting a 2 wt% surfactant solution with heptane; calculated based on the partition-bifunctional model (squares) and based on the segregation-bifunctional model (triangles)

obtained via high-temperature gas chromatography (Silver & Kalinoski, 1992). The alcohol used to synthesize these surfactants was C_{11} alcohol (Exxal™ 11), also donated by ExxonMobil Chemical Company. The typical composition of C_{11} alcohol consists of 6.7% C_{10} alcohol, 87.0% C_{11} alcohol, and 6.3% C_{12} alcohol, and an average of 2.2 CH_3— branches per chain.

Two reference AEs, previously used in the literature, were donated by BASF North America. These surfactants can be nominally represented as C_8E_4 (Dehydol® OD4, ~100%) and C_9E_5 (Dehydol® OD5, ~100%) (Zarate-Muñoz et al., 2016).

Heptane (≥99.5%) was purchased from Caledon Laboratory Chemicals (Georgetown, ON). Reagent

grade sodium chloride was purchased from Bioshop Canada Inc. (Burlington, ON). All chemicals were used as received.

Methods

Phase behavior: salinity scans

For surfactants $C_{11}E_{3\_BR}$, $C_{11}E_{5\_BR}$, and $C_{11}E_{7\_BR}$, the values of σ_{app} were obtained via salinity scans at different temperatures using a high-throughput robotic system through a third-party characterization facility (Natali, 2019). The scans were conducted using NaCl as the electrolyte, *n*-heptane as the oil phase, and using each surfactant alone (i.e., no combinations with reference surfactants). The aqueous-to-oil phase volume ratio was maintained at 1:1. The values of σ_{app} were calculated using the same method explained earlier with the example of Figure 5, considering the temperature at which the S^* was obtained.

For surfactants $C_{11}E_{3\_NR}$, $C_{11}E_{5\_NR}$, and $C_{11}E_{7\_NR}$, the values of σ_{app} were obtained in-house, using room temperature ($T = 25^{\circ}C$) salinity scans. To determine the phase inversion (optimal) salinity, S^*, salinity scans were produced by mixing 5 ml of *n*-heptane (oil phase) and 5 ml of the aqueous phase in 15-ml flat bottom test tubes. Figure 5 presents an example of the salinity scans for $C_{11}E_{5\_NR}$. For $C_{11}E_{3\_NR}$, being too hydrophobic to produce an S^* at room temperature, salinity scans were conducted with a mixture of 50 mol% $C_{11}E_{3\_NR}$ and 50 mol% C_8E_4 (reference surfactant). The use of linear mixing rules in test + reference surfactant (including the reference surfactants employed in this work) mixtures employed in determining σ (Cc) has been cross-validated with several nonionic surfactant systems (Zarate-Muñoz et al., 2016). Using the linear mixing rule, $\sigma_{app,mix} = 0.5{\cdot}\sigma_{app,C11E3\_NR} + 0.5{\cdot}\sigma_{app,C8E4}$, where $\sigma_{app,mix}$ is determined from the salinity scan (illustrated for the scans of Figure 5). The value of $\sigma_{app,C8E4}$ was determined via $T = 25^{\circ}C$ salinity scans with 20, 10, and 5 wt% C_8E_4 and heptane, obtaining values $\sigma_{app,C8E4}$ of -1.4, -2.1, and -3.3 at each of these concentrations. No phase inversion was observed with a 2 wt% C_8E_4–heptane system at room temperature to obtain $\sigma_{app,C8E4}$. For $C_{11}E_{7\_NR}$, this surfactant is too hydrophilic to produce an S^* at room temperature; thus, equimolar mixtures of $C_{11}E_{7\_NR}$ and $C_{11}E_{3\_NR}$ were used to produce systems that experience salinity-induced phase inversion at room temperature, then $\sigma_{app,C11E7\_NR} = 2\sigma_{app,mix} - \sigma_{app,C11E3\_NR}$.

It should be clarified that although Figure 5 shows pictures where middle phases are identified (or at least the closest salinity to a middle phase system) as the points of inversion (S^*), the reality is that one can obtain several middle phase systems, depending on the step used in the salinity scan. In the absence of middle phases, a more representative value of S^* was obtained by fitting the entire salinity scan using the NAC model, as described in the literature (Ghayour & Acosta, 2019; Zarate-Muñoz et al., 2016).

Polar oil characterization for the C_{11} alcohol

Salinity phase scans were conducted at room temperature to obtain the Km_0 value for the alcohol, using 16 wt % C_9E_5 as reference surfactant and heptane as the oil phase mixed with various volume fractions of the C_{11} alcohol. This is the same procedure used by Ghayour and Acosta (Ghayour & Acosta, 2019, 2020). Figure 7 presents the phase inversion (S^*) salinities obtained with these systems as a function of the volume fraction of C_{11} alcohol added to the oil phase. The method to fit the polar oil (bifunctional) model to the S^* versus alcohol content data has been described elsewhere

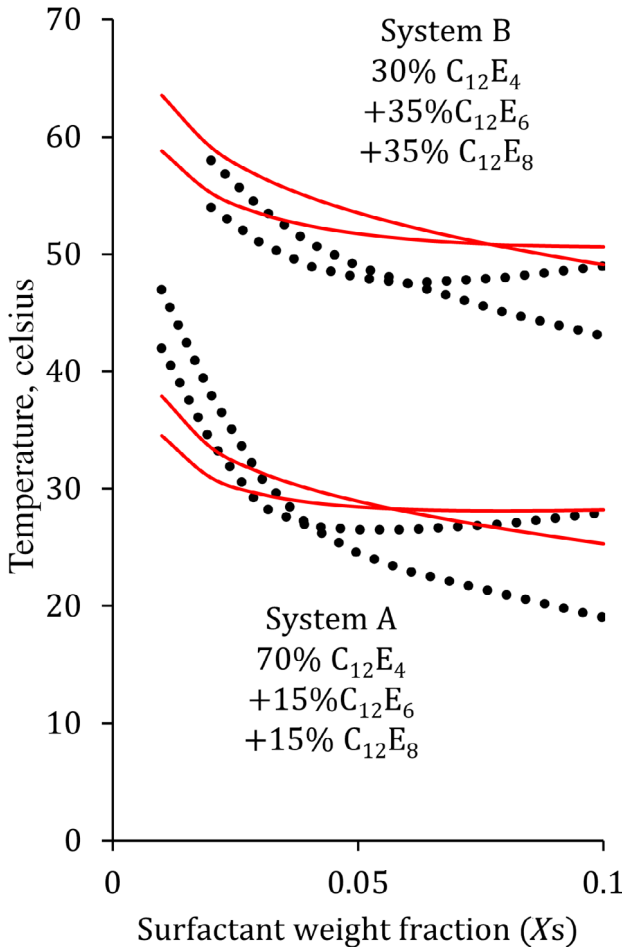

FIGURE 10 Fish phase diagrams for mixtures of monodisperse $C_{12}E_4$, $C_{12}E_6$, and $C_{12}E_8$ surfactants evaluated experimentally by Kunieda and Shinoda (1985) (dashed line). The solid lines are the phase boundary predictions obtained with the hydrophile–lipophile balance (HLD)–net-average curvature (NAC) and the segregation-bifunctional algorithm of Figure 3. An example calculation for $X_S = 0.02$ is shown in Section II of File S1

(Ghayour & Acosta, 2019, 2020). In this case, the only difference is that the fit of the bifunctional model required various restrictions to be consistent with the algorithm of Figure 3. Specifically, the bifunctional fit needs to use $\sigma_{C11alcohol} = 5.5$ obtained from the linear group contribution, $EACN_{C11alcohol} = -20$, and $q_{max,C11alcohol} = 0.7$. Therefore, the only adjustable parameter left to fit is $K_{m,C11alcohol}$. The fit (solid line) in Figure 7 uses $K_{m,C11alcohol} = 0.53\ M^{-1}$, which was used in the algorithm of Figure 3 to predict σ_{app} for the six AEs considered in this work.

RESULTS AND DISCUSSION

Experimental versus bifunctional model σ_{app} for broad and narrow range AEs

Figure 8 presents the experimentally determined apparent sigma (σ_{app}) values as a function of surfactant concentration for the six surfactant systems explored in this work. Figure 8 includes the σ_{app} predicted from the segregation-bifunctional AE algorithm of Figure 3, with the Langmuir Km constant estimated using Equation (A.4), $K_{m,j<7} = Km_0 \cdot 10^{(fl \cdot j)}$, with $Km_0 = 0.53\ M^{-1}$ and $fl = 0.42$. The results from the partition-bifunctional model are also displayed in Figure 8. The predictions from the partition-bifunctional model used the calculations of Section I of File S1, and Equations (A.6) through (A.10) and Equations (A.13) through (A.15) of the algorithm of Figure 3.

Before discussing the predictions, let us compare the experimental trends. BR AEs show greater dependence of σ_{app} with surfactant concentration as compared to narrow-range AEs. Similarly, lower average EO numbers tend to produce greater σ_{app} dependence on surfactant concentration. These trends are consistent with the partition concept illustrated in Figure 2, specifically that systems with more hydrophobic components (C_nE_j, with $j = 0$, 1, 2, and 3) will experience more partition and changes in oil composition and interface composition.

The trends observed in the experiments are also reflected in the predictions of the segregation-bifunctional and partition-bifunctional models. According to Figure 8, the partition-bifunctional model seems, in principle, accurate for $C_{11}E_3$ surfactants; however, the heptane–water partition coefficient of C_{11} alcohol had to be adjusted to $10^{4.5}$ to get a suitable approximation to all the experimental data. This adjusted partition coefficient is close to a value estimated for C_{11} alcohol between water and isooctane ($10^{4.4}$) obtained from the thermodynamic analysis of Ghoulam et al. (2002). For the case of the segregation-bifunctional model, no value was adjusted. The value of Km_0 used in the algorithm of Figure 3 was found independently via the polar oil study in Figure 7; thus, the segregation-bifunctional model is fully predictive. The segregation-bifunctional model does a reasonable prediction of the apparent sigma for $C_{11}E_5$ and $C_{11}E_7$ surfactants. The average deviation obtained with the partition-bifunctional model is 0.43 units of sigma, and with the segregation-bifunctional model is 0.47 units of sigma. The accuracy of the two versions of the bifunctional model is directly connected to the predicted ethoxy group distribution after contact with the oil phase, presented in Figure 9.

Figure 9 presents the ethoxymer distribution in the surfactant pseudophase before (initial, measured via GC) and after adding heptane to a 2 wt% surfactant solution where the distribution was predicted via the bifunctional model (partition and segregation versions). Logistical limitations prevented us from measuring the final EO distribution. Zarate-Muñoz et al. (2015) obtained the final EO distribution after contacting C_9E_5 and $C_{13}E_6$ with decalin (EACN ~6.3) and noted that in both cases, the signals for ethoxymers $j = 1$, 2, 3 were missing or barely noticeable, consistent with the curves in Figure 9.

Graciaa et al. used a version of the partition model (same three-compartment balance used in our work, just a different set of partition expressions and method of solution) to determine the EO in the surfactant pseudophase (Graciaa et al., 1983). In their work, they observed that an NPE ethoxylate with an average of five EO units (NPE5) when set in contact with isooctane then produced a shift in the peak distribution to about six EO units, which was consistent between measurements and model prediction. However, compared to the measured distribution after contacting the oil, the partition model appears to have overpredicted the removal of NPE1, NPE2, and NPE3 from the surfactant pseudophase. This observation is consistent with the trends observed with the partition model distributions shown in Figure 9. For $C_{11}E_{3\_BR}$ and $C_{11}E_{3\_NR}$, at least when compared to the segregation model, the partition model seems to overpredict the removal of $C_{11}E_2$ to $C_{11}E_5$ ethoxymers. One must keep in mind that the distribution is largely dependent on the value of the oil–water partition coefficient for the alcohol ($K_{o/w}$). Using lower values of this partition constant leads to an increase in the content of $C_{11}E_2$ to $C_{11}E_5$ in the surfactant pseudophase, especially for the $C_{11}E_{3\text{-}BR}$ and $C_{11}E_{3\text{-}NR}$ surfactants. Overall, the general shape of the segregation model distribution is consistent with the partition model, except that the segregation model tends to produce a small discontinuity around $C_{11}E_7$ because this is the cutoff point for the nonpartitioning species. Despite this small discontinuity, the predictions are useful to understand the trends in changes of composition. A preliminary version of the segregation model used a cutoff point of $C_{11}E_9$ for nonpartitioning species, and in that case, large discontinuities in the EO distributions were observed around $C_{11}E_9$.

Predicted fish phase diagrams with HLD–NAC and the bifunctional AE model

Fish or phase map diagrams are useful to determine the proximity of a formulation to the phase inversion and the potential effect that dilution might have on the system's phase behavior or in the system's solubilization capacity (Yuan et al., 2010). Kunieda and Shinoda explored the role of polydispersity on the location and shape of the fish phase diagram. These researchers used mixtures of monodispersed $C_{12}E_4$, $C_{12}E_6$, and $C_{12}E_8$ to simulate polydisperse products and generate fish phase diagrams (Kunieda & Shinoda, 1985). In this work, we combined the segregation-bifunctional model with the HLD-NAC model to compare predicted fish phase diagram boundaries with the experimental boundaries determined by Kunieda and Shinoda. To undertake this simulation, the initial composition set by Kunieda and Shinoda was used as an input. The value of Km_{12_0} was approximated to $Km_{11\_0} = 0.53\ M^{-1}$. Section II of File S1 has a step-by-step example of the implementation of the segregation-bifunctional model to calculate the HLD values and the application of the NAC equations to determine the temperature phase boundaries.

The phase boundaries of SOW systems from surfactant + solubilized oil in water (o/w) or Type I microemulsions (μEs), to bicontinuous Type III (3 phases) or Type IV (1 phase) μEs, to surfactant + solubilized water in oil (w/o) or Type II μEs, can be estimated using the NAC model. According to a simplified form of the NAC model, the $HLD_{I–III}$ and $HLD_{II–III}$ boundaries are as follows (Acosta, 2020):

$$HLD_{I-III} = 2L\left(\frac{1}{R_{W,max}} - \frac{1}{\xi}\right) \quad (2)$$

$$HLD_{III-II} = 2L\left(\frac{1}{\xi} - \frac{1}{R_{O,max}}\right) \quad (3)$$

where L is the surfactant tail length parameter, estimated as 1.4*extended tail length (Acosta, 2008). For a linear C_{12} surfactant, $L = 23$ Å (Acosta & Sundar, 2019). The term ξ is the characteristic length or maximum solubilization capacity of the μE system. For μEs produced with linear monodisperse C_nE_j and n-alkanes, the characteristic length can be estimated as $\xi = 67\ Å \cdot e^{(0.44 \cdot n)}/(EACN \cdot j)$ (Acosta, 2008). The oil used in the work of Kunieda and Shinoda was n-heptane (EACN = 7), the surfactant had a C_{12} ($n = 12$) tail. As illustrated in Section II of File S1, the value of the characteristic length for the mixture was determined with the known composition of the surfactant pseudophase (X_j), and the characteristic length that corresponds to each ethoxymer (ξ_j) such that $\xi = \Sigma(\xi_j)^*(X_j)$. The last terms needed for Equations 2 and 3 are the solubilization radii of the entire oil ($R_{O,max}$) and the entire aqueous phase ($R_{W,max}$) in the system. The radii can be calculated as $R_{O,max} = 3 \cdot (v_S/a_S)\varphi_O/\varphi_S$ and $R_{W,max} = 3 \cdot (v_S/a_S)\varphi_W/\varphi_S$. Kuneida and Shinoda used an oil/water weight ratio of 1:1, and the surfactant concentration was expressed as mass fraction of the entire system (x_S). To calculate volume fractions of surfactant (φ_S), oil (φ_O), and water (φ_W) in the entire system, for a given surfactant weight fraction in the entire system (x_S), the densities of water and surfactant were both taken as 1 g/ml, and the density of heptane as 0.68 g/ml. The term v_S/a_S is the ratio between the volume and interfacial area of a surfactant molecule. The values of $(v_S/a_S)_j$ for each ethoxymer were obtained from their molecular weight, density (1 g/ml), and the surfactant area per molecule obtained from Rosen's tables (Rosen & Kunjappu, 2012) and listed in Section II of File S1. For the entire surfactant pseudophase, $(v_S/a_S) = \Sigma X_j^*(v_S/a_S)_j$.

To undertake the prediction of the fish phase diagram, for a given x_S, then φ_S, φ_O, φ_W, $R_{W,max}$, and $R_{O,max}$ are calculated, and given the values of the other terms in Equations 2 and 3, then HLD_{I-III} and HLD_{III-II} are calculated. To use the bifunctional AE algorithm of Figure 3 to find σ_{app}, the composition of the initial mixture and φ_S were used to obtain the initial aqueous concentrations C_{nj}, considering that the water-to-oil volume ratio is $r_{W/O} = 0.68$ (from water/oil weight ratio = 1/1 and the densities of the two phases). With the HLD boundaries ($HLD_{I–III}$ and $HLD_{III–II}$) and σ_{app}, the boundary temperature can be calculated from Equation (1) as $T_{boundary} = (HLD_{boundary} + k \cdot EACN - \sigma_{app} - b \cdot S)/c_T + 25°C$. Using the k, b, and c_T values listed in the algorithm of Figure 3, and considering that Kunieda and Shinoda used heptane as oil (EACN = 7) and did not report any salt addition ($S = 0$), the boundary temperatures (I–III and III–II) were calculated as a function of φ_S.

Figure 10 summarizes the prediction of the HLD-NAC + segregation-bifunctional model, represented by solid lines, and the experimental boundaries obtained by Kunieda and Shinoda for systems A (70 wt% $C_{12}E_4$, 15 wt% $C_{12}E_6$, 15 wt% $C_{12}E_8$) and B (30 wt% $C_{12}E_4$, 35 wt% $C_{12}E_6$, and 35 wt% $C_{12}E_8$), represented by dotted lines. Overall, the experimental trends are represented by the predictions, including the curvature of the boundary lines. The average deviation between the predicted and experimental transition temperatures for both systems is 3.5°C, which is equivalent to about 0.06*3.5 = 0.21 HLD units, which can be interpreted as 0.21σ units. The predicted cross or "X" point between III and IV μEs for systems A and B occurs at higher surfactant concentrations than those observed in the experiments. This means that the estimated characteristic lengths (ξ) are smaller than the experimental ones. This deviation is likely associated with the surfactant $C_{12}E_4$ serving as a lipophilic linker known to increase

the characteristic length of μEs (Ghayour & Acosta, 2019).

Practical implications and areas for future research

The issue of alkyl ethoxylates partitioning into the oil and its impact on the hydrophobicity of the surfactant pseudophase was identified and studied in the early 1980s (Graciaa et al., 1983; Harusawa & Tanaka, 1981; Kunieda & Shinoda, 1985). However, finding a way of accounting for oil partitioning or predicting its impact has become an emerging issue in the implementation of the HLD and the HLD-NAC frameworks. Recent industry-led presentations at American Oil Chemists Society (AOCS) meetings have introduced experimental and modeling approaches to account for these effects and their impact on surfactant formulation (Dado & Lang, 2021; Ghayour, 2021; Natali & Acosta, 2021). There are now clear connections between phase inversion conditions (HLD = 0) and the performance of formulations in detergency (Phaodee & Sabatini, 2020; Raney et al., 1987; Raney & Benson, 1990; Saito et al., 1985; Thompson, 1994; Tongcumpou et al., 2003); the performance of formulations used to decontaminate oil-impacted soils (Acosta & Quraishi, 2014; Childs et al., 2005; Kibbey & Chen, 2008; Quraishi et al., 2015); the performance of phase inversion methods to produce nanoemulsions (McClements, 2011; Solans et al., 2005); the performance of demulsifiers (Rondón et al., 2006); the formation and breaking of emulsions (Kiran & Acosta, 2015); the formulation with fragrances (Bouton et al., 2009; Tchakalova & Fieber, 2012); the formulation of skin cleaning products (Acosta, 2020), among many others. The connection between the phase inversion conditions and optimal enhanced oil recovery is well known and covered in the classic textbook of Bourrel and Schecter (1988).

The increasing evidence of the practical use of the HLD and HLD–NAC frameworks has prompted more frequent requests for values of sigma from surfactant manufacturers. However, what value of sigma (determined at oil/water ratios ~1) could an alkyl ethoxylate manufacturer provide if the value depends on the surfactant concentration used in the aqueous formulation? This work provides various ways of answering that question. The first answer is that the important concentration is the oil-equivalent concentration after discounting for the CMC. For example, if a surfactant is used at a concentration of 0.1 wt% in water, and the mixed CMC is 0.01 wt%, and 1 kg of the aqueous formulation is contacted with 10 g of oil, then the oil-equivalent concentration is (0.1–0.01 wt%)*1000 g/10 g ~ 9 wt% of equivalent concentration in the oil. If the oil content in the system is 100 g instead, then the oil-equivalent concentration is 0.9 wt%. In the first case, a sigma value obtained at about 9 wt% of surfactant is relevant, but in the second case, a sigma value obtained at 0.9 wt% is the relevant one.

The second implication of this work is that if the surfactant has a low free alcohol content and low content of E_1 to E_5 ethoxymers, then the sigma value is expected to be largely independent of surfactant concentration. Thus, alkyl ethoxylates with an average ethoxy group number of 7 or more are less likely to experience concentration-dependent sigma values.

The third implication of the work is that the concentration-dependent values of sigma can be estimated from the ethoxy group distribution of the polydisperse alkyl ethoxylate, which can be determined using gas or liquid chromatography. This concentration dependence is a function of the oil used. When using the segregation-bifunctional model, the effect of oil can be accounted for by repeating the experiment of Figure 7, but in the presence of the oil of interest, and obtaining the value of the segregation constant for the alcohol (Km_0). Once this value is obtained, and with known ethoxy distribution, the entire values of sigma versus concentration can be predicted. If one wants to use the partition-bifunctional model, the challenge is to obtain a good estimate for the oil–water partition coefficient of the alcohol ($K_{o/w}$). If the oil phase is well characterized, perhaps the value could be estimated using thermodynamic models like UNIFAC. $K_{o/w}$ could be measured using chromatography or other analytical techniques to detect alcohol concentration in the oil phase. If access to instrumentation or to a thermodynamic model validated for the oil of interest is limited, then the segregation-bifunctional model is a more accessible route because it only needs the phase scan study shown in Figure 7.

The combination of the segregation-bifunctional and NAC predicts μE phase boundaries for mixtures of alkyl ethoxylates that deviate, on average, about ±0.2 HLD units from the experimental values. When considering polydisperse alkyl ethoxylates, both the segregation-bifunctional and the partition-bifunctional models predict the values of sigma that are within ±0.5 sigma units of the experimental values. The reader is warned that, in practice, the predicted σ should be used to narrow down the surfactant selection and the experimental conditions used to test/validate candidate formulations. Around the phase inversion, a ±0.5 uncertainty in σ is significant because in the −0.5 to +0.5 HLD range, there are substantial changes in system properties, for example, interfacial tension and emulsion stability can vary by orders of magnitude.

ACKNOWLEDGMENTS

The support of ExxonMobil Chemicals Company is acknowledged and also the permission of the company to publish this work.

CONFLICT OF INTEREST

The authors declare that they have no conflict of interest.

AUTHOR CONTRIBUTIONS

Edgar Acosta: Conceptualization, Software, Methodology, Validation, Formal analysis, Investigation, Data Curation, Writing Original Draft, Writing- review and Editing, Visualization. **Sanja Natali:** Conceptualization, Methodology, Formal analysis, Investigation, Data Curation, Writing- review and Editing, Funding.

ETHICS STATEMENT

This research falls outside of human or animal studies and institutional ethical approval was not required.

ORCID

Edgar Acosta https://orcid.org/0000-0002-8186-1093

REFERENCES

Acosta EJ. The HLD-NAC equation of state for microemulsions formulated with nonionic alcohol ethoxylate and alkylphenol ethoxylate surfactants. Colloids Surf A Physicochem Eng Asp. 2008;320:193–204. https://doi.org/10.1016/j.colsurfa.2008.01.049

Acosta EJ. Engineering cosmetics using the net-average-curvature (NAC) model. Curr Opin Colloid Interface Sci. 2020;48:149–67. https://doi.org/10.1016/j.cocis.2020.05.005

Acosta EJ, Quraishi S. Surfactant technologies for remediation of oil spills. In: Ponisseril S, Patra P, Farinato RS, Papadopoulos K, editors. Oil spill remediation: colloid chemistry-based principles and solutions. 1st ed. Hoboken, NJ: Wiley; 2014. p. 317–58. https://doi.org/10.1002/9781118825662.ch15

Acosta EJ, Sundar S. How to formulate biobased surfactants through the HLD-NAC model. In: Hayes D, Solaiman D, Ashby R, editors. Biobased surfactants. 2nd ed. London, England: AOCS Press; 2019. p. 471–510. https://doi.org/10.1016/B978-0-12-812705-6.00015-0

Acosta EJ, Yuan JS, Bhakta AS. The characteristic curvature of ionic surfactants. J Surfactant Deterg. 2008;11:145–58. https://doi.org/10.1007/s11743-008-1065-7

Antón RE, Andérez JM, Bracho C, Vejar F, Salager J-L. Practical surfactant mixing rules based on the attainment of microemulsion-oil-water three-phase behavior systems. Adv Polymer Sci. 2008;218(1):83–113. https://doi.org/10.1007/12_2008_163

Aubry JM, Ontiveros JF, Salager JL, Nardello-Rataj V. Use of the normalized hydrophilic-lipophilic-deviation (HLDN) equation for determining the equivalent alkane carbon number (EACN) of oils and the preferred alkane carbon number (PACN) of nonionic surfactants by the fish-tail method (FTM). Adv Colloid Interface Sci. 2020;276:1–24. https://doi.org/10.1016/j.cis.2019.102099

Bourrel M, Schechter RS. Microemulsions and related systems. New York, NY: Marcel Dekker; 1988.

Bouton F, Durand M, Nardello-Rataj V, Serry M, Aubry JM. Classification of terpene oils using the fish diagrams and the equivalent alkane carbon (EACN) scale. Colloids Surf A Physicochem Eng Asp. 2009;338:142–7. https://doi.org/10.1016/j.colsurfa.2008.05.027

Boza-Troncoso A, Acosta EJ. The UNIFAC model and the partition of alkyl and alkylphenol ethoxylate surfactants in the excess phases of middle phase microemulsions. Fluid Phase Equilibria. 2015;397:117–25. https://doi.org/10.1016/j.fluid.2015.03.035

Boza-Troncoso A, Acosta EJ. Formulating nonionic detergents via the integrated free energy model. J Surfactant Deterg. 2019;22:1023–37. https://doi.org/10.1002/jsde.12322

Childs JD, Acosta E, Scamehorn JF, Sabatini DA. Surfactant-enhanced treatment of oil-based drill cuttings. J Energy Resour Technol Trans ASME. 2005;127:153–62. https://doi.org/10.1115/1.1879044

Choi F, Zarate-Muñoz S, Acosta EJ. Prediction of cloud point curves of alkyl Ethoxylates with the hydrophilic–lipophilic-difference and net-average-curvature (HLD-NAC) framework. J Surfactant Deterg. 2019;22:973–82. https://doi.org/10.1002/jsde.12304

Dado, G., & Lang, R. (2021). HLD modeling of the concentration-dependent behavior of nonionic surfactant mixtures. American Oil Chemists Society 2021 Annual Meeting Available from: https://680c20bb37fdff6e3d02-e9a5ae3b0fb0e09eedd089239cefb046.ssl.cf1.rackcdn.com/1597798-1014438-003.pdf

Ghayour, A. (2021). Measuring the characteristic curvature of commercial Ethoxylated nonionic surfactants. American Oil Chemists Society. 2021 Annual Meeting. Available from: https://680c20bb37fdff6e3d02-e9a5ae3b0fb0e09eedd089239cefb046.ssl.cf1.rackcdn.com//1597785-1253916-001.pdf

Ghayour A, Acosta E. Characterizing the oil-like and surfactant-like behavior of polar oils. Langmuir. 2019;35:15038–50. https://doi.org/10.1021/acs.langmuir.9b02732

Ghayour A, Acosta EJ. Erratum: characterizing the oil-like and surfactant-like behavior of polar oils. Langmuir. 2020;36:3276–3277l. https://doi.org/10.1021/acs.langmuir.0c00510

Ghoulam MB, Moatadid N, Graciaa A, Lachaise J. Effects of oxyethylene chain length and temperature on partitioning of homogeneous polyoxyethylene nonionic surfactants between water and isooctane. Langmuir. 2002;18:4367–71. https://doi.org/10.1021/la0117707

Goe SK. Tuning the polydispersity of alcohol ethoxylates for enhanced oily soil removal. J Surfactant Deterg. 1998;1:539–45. https://doi.org/10.1007/s11743-998-0056-9

Graciaa A, Andérez J, Bracho C, Lachaise J, Salager J-L, Tolosa L, et al. The selective partitioning of the oligomers of polyethoxylated surfactant mixtures between interface and oil and water bulk phases. Adv Colloid Interface Sci. 2006;123–126:63–73. https://doi.org/10.1016/j.cis.2006.05.015

Graciaa A, Lachaise J, Sayous JG, Grenier P, Yiv S, Schechter RS, et al. The partitioning of complex surfactant mixtures between oil/water/microemulsion phases at high surfactant concentrations. J Colloid Interface Sci. 1983;93:474–86. https://doi.org/10.1016/0021-9797(83)90431-9

Griffin WC. Calculation of HLB values of non-ionic surfactants. J Soc Cosmet Chem. 1954;5:249–56.

Harusawa F, Nakajima H, Tanaka F. The hydrophile-lipophile balance of mixed nonionic surfactants. J Soc Cosmet Chem. 1982;33:115–29.

Harusawa F, Tanaka M. Mixed micelle formation in two-phase systems. J Phys Chem. 1981;85:882–5. https://doi.org/10.1021/j150607a029

Kibbey TCG, Chen L. Phase volume effects in the sub- and super-CMC partitioning of nonionic surfactant mixtures between water and immiscible organic liquids. Colloids Surf A Physicochem Eng Asp. 2008;326:73–82. https://doi.org/10.1016/j.colsurfa.2008.05.018

Kiran SK, Acosta EJ. HLD–NAC and the formation and stability of emulsions near the phase inversion point. Ind Eng Chem Res. 2015;54:6467–79. https://doi.org/10.1021/acs.iecr.5b00382

Kiran SK, Acosta EJ, Moran K. Evaluating the hydrophilic-lipophilic nature of asphaltenic oils and naphthenic amphiphiles using microemulsion models. J Colloid Interface Sci. 2009;336:304–13. https://doi.org/10.1016/j.jcis.2009.03.053

Kunieda H, Shinoda K. Evaluation of the hydrophile-lipophile balance (HLB) of nonionic surfactants. I. Multisurfactant systems. J Colloid Interface Sci. 1985;107:107–21. https://doi.org/10.1016/0021-9797(85)90154-7

Marketsandmarkets. (2020). Ethoxylates market by type. Market research report Available from: https://www.marketsandmarkets.com/Market-Reports/ethoxylates-market-124534176.html

Márquez N, Bravo B, Chávez G, Ysambertt F, Salager JL. Analysis of polyethoxylated surfactants in microemulsion-oil-water systems. Anal Chim Acta. 2000;405:267–75. https://doi.org/10.1016/S0003-2670(99)00759-X

McClements DJ. Edible nanoemulsions: fabrication, properties, and functional performance. Soft Matter. 2011;7:2297–316. https://doi.org/10.1039/c0sm00549e

Natali, S. (2019). Branched alcohols contribution to surfactant characteristic curvature and other HLD-NAC parameters. American Oil Chemists' Society Annual Meeting 2019.

Natali, S., & Acosta, E. (2019). The effect of surfactant alkyl structure on cold water detergency. CESIO Poster. Available from: https://www.exxonmobilchemical.com/-/media/amer/us/chem/micsellaneous/cesio_2019_poster.pdf

Natali, S., & Acosta, E. (2021). Effect of alkyl Ethoxylates polydispersity on the hydrophobicity with surfactant concentration. American Oil Chemists Society 2021 Annual Meeting. Available from: https://www.eventscribeapp.com/live/videoPlayer.asp?lsfp=dGdFejZFS2JyUEw4VVJDT1hOTmRRakUrT0RDUkZqRzdGMENCYloraURNOD0=

Phaodee P, Sabatini DA. Effect of surfactant systems, alcohol types, and salinity on cold-water detergency of triacylglycerol semisolid soil. Part II. J Surfactants Deterg. 2020;23:423–32. https://doi.org/10.1002/jsde.12374

Quraishi S, Bussmann M, Acosta E. Capillary curves for ex-situ washing of oil-coated particles. J Surfactant Deterg. 2015;18:811–23. https://doi.org/10.1007/s11743-015-1704-8

Raney KH, Benson HL. The effect of polar soil components on the phase inversion temperature and optimum detergency conditions. J Am Oil Chem Soc. 1990;67:722–9. https://doi.org/10.1007/BF02540479

Raney KH, Benton WJ, Miller CA. Optimum detergency conditions with nonionic surfactants. I. Ternary water-surfactant-hydrocarbon systems. J Colloid Interface Sci. 1987;117:282–90. https://doi.org/10.1016/0021-9797(87)90192-5

Rondón M, Bouriat P, Lachaise J, Salager JL. Breaking of water-in-crude oil emulsions. 1. Physicochemical phenomenology of Demulsifier action. Energy Fuel. 2006;20:1600–4. https://doi.org/10.1021/ef060017o

Rosen MJ, Kunjappu JT. Surfactants and interfacial phenomena. 4th ed. Hoboken, NJ: John Wiley & Sons, Inc; 2012. https://doi.org/10.1002/9781118228920

Saito M, Otani M, Yabe A. Work of adhesion of oily dirt and correlation with Washability. Textile Res J. 1985;55:157–64. https://doi.org/10.1177/004051758505500304

Salager JL. Physico-chemical properties of surfactant– water–oil mixtures: phase behavior, microemulsion formation and interfacial tension. Austin, TX: University of Texas; 1977.

Salager JL. Formulation concepts for the emulsion maker. In: Nielloud F, Marti-Mestres G, editors. Pharmaceutical emulsions and suspensions. New York, NY: Marcel Dekker; 2000. p. 19–72. https://doi.org/10.1201/b14005-3

Salager JL, Antón RE, Sabatini DA, Harwell JH, Acosta EJ, Tolosa LI. Enhancing solubilization in microemulsions - state of the art and current trends. J Surfactant Deterg. 2005;8:3–21. https://doi.org/10.1007/s11743-005-0328-4

Salager JL, Forgiarini AM, Bullon J. How to attain ultralow interfacial tension and three-phase behavior with surfactant formulation for enhanced oil recovery: a review. Part 1. Optimum formulation for simple surfactant-oil-water ternary systems. J Surfactant Deterg. 2013;16:449–72. https://doi.org/10.1007/s11743-013-1470-4

Salager JL, Marquez N, Graciaa A, Lachaise J. Partitioning of ethoxylated octylphenol surfactants in microemulsion-oil-water systems: influence of temperature and relation between partitioning coefficient and physicochemical formulation. Langmuir. 2000;16:5534–9. https://doi.org/10.1021/la9905517

Salager JL, Morgan JC, Schechter RS, Wade WH, Vasquez E. Optimum formulation of surfactant/water/oil systems for minimum interfacial tension or phase behavior. Soc Petroleum Eng J. 1979;19:107–15. https://doi.org/10.2118/7054-PA

Silver AH, Kalinoski HT. Comparison of high-temperature gas chromatography and CO_2 supercritical fluid chromatography for the analysis of alcohol ethoxylates. J Am Oil Chem Soc. 1992;69:599–608. https://doi.org/10.1007/BF02635796

Solans C, Izquierdo P, Nolla J, Azemar N, Garcia-Celma MJ. Nano-emulsions. Curr Opin Colloid Interface Sci. 2005;10:102–10. https://doi.org/10.1016/j.cocis.2005.06.004

Tchakalova V, Fieber W. Classification of fragrances and fragrance mixtures based on interfacial solubilization. J Surfactant Deterg. 2012;15:167–77. https://doi.org/10.1007/s11743-011-1295-y

Thompson L. The role of oil detachment mechanisms in determining optimum detergency conditions. J Colloid Interface Sci. 1994;163:61–73. https://doi.org/10.1006/jcis.1994.1080

Tongcumpou C, Acosta EJ, Quencer LB, Joseph AF, Scamehorn JF, Sabatini DA, et al. Microemulsion formation and detergency with oily soils: I. Phase behavior and interfacial tension. J Surfactants Deterg. 2003;6:191–203. https://doi.org/10.1007/s11743-003-0262-5

Warr GG, Grieser F, Healy TW. Distribution of polydisperse nonionic surfactants between oil and water. J Phys Chem. 1983;87:4520–4. https://doi.org/10.1021/j100245a036

Yuan JS, Yip A, Nguyen N, Chu J, Wen XY, Acosta EJ. Effect of surfactant concentration on transdermal lidocaine delivery with linker microemulsions. Int J Pharm. 2010;392:274–84. https://doi.org/10.1016/j.ijpharm.2010.03.051

Zarate-Muñoz S, Boza-Troncoso A, Acosta EJ. The cloud point of alkyl Ethoxylates and its prediction with the hydrophilic-lipophilic difference (HLD) framework. Langmuir. 2015;31:12000–8. https://doi.org/10.1021/acs.langmuir.5b03064

Zarate-Muñoz S, Texeira De Vasconcelos F, Myint-Myat K, Minchom J, Acosta EJ. A simplified methodology to measure the characteristic curvature (Cc) of alkyl ethoxylate nonionic surfactants. J Surfactant Deterg. 2016;19:249–63. https://doi.org/10.1007/s11743-016-1787-x

SUPPORTING INFORMATION

Additional supporting information may be found in the online version of the article at the publisher's website.

How to cite this article: Acosta E, Natali S. Effect of surfactant concentration on the hydrophobicity of polydisperse alkyl ethoxylates. J Surfact Deterg. 2022;25:79–94. https://doi.org/10.1002/jsde.12548